

Organic & Biomolecular Chemistry

Accepted Manuscript



This is an *Accepted Manuscript*, which has been through the Royal Society of Chemistry peer review process and has been accepted for publication.

Accepted Manuscripts are published online shortly after acceptance, before technical editing, formatting and proof reading. Using this free service, authors can make their results available to the community, in citable form, before we publish the edited article. We will replace this *Accepted Manuscript* with the edited and formatted *Advance Article* as soon as it is available.

You can find more information about *Accepted Manuscripts* in the [Information for Authors](#).

Please note that technical editing may introduce minor changes to the text and/or graphics, which may alter content. The journal's standard [Terms & Conditions](#) and the [Ethical guidelines](#) still apply. In no event shall the Royal Society of Chemistry be held responsible for any errors or omissions in this *Accepted Manuscript* or any consequences arising from the use of any information it contains.

Accurate *ab initio* calculations of O–H---O and O–H--- \bar{O} proton chemical shifts: towards elucidation of the nature of the hydrogen bond and prediction of hydrogen bond distances[†]

Michael Siskos,^{*a} Andreas G. Tzakos^a and Ioannis P. Gerothanassis^{*a,b}

^a Section of Organic Chemistry and Biochemistry, Department of Chemistry, University of Ioannina, Ioannina, GR 45110, Greece. E-mail: msiskos@cc.uoi.gr, igeroth@uoi.gr, agtzakos@gmail.com; Fax: (+30) 26510-08799; Tel: (+30) 26510-08389

^b H.E.J. Research Institute of Chemistry, University of Karachi, Karachi 75270, Pakistan

[†]Electronic supplementary information (ESI) available: Fig.S1. Plot of the difference in the NBO charge densities, $\Delta Q \times 10^3$, of the two oxygens participating in the intramolecular O–H---O hydrogen bond. Fig.S2. Plot of calculated Wiberg bond order of the C2=O1 group of the intramolecular CO---H(O) hydrogen bond. Table S1. Structural data and ¹H NMR chemical shifts for selected compounds. Table S2. Wiberg charge density within the intramolecular hydrogen bonded moiety. For ESI see DOI: 10.1039/XXXX

Abstract: The inability to determine precisely the location of labile protons in X-ray molecular structures has been a key barrier to progress in many areas of molecular sciences. We report an approach for predicting hydrogen bond distances beyond the limits of X-ray crystallography based on accurate *ab initio* calculations of O–H---O proton chemical shifts, using a combination of DFT and contactor-like polarizable continuum model (PCM). Very good linear correlation between experimental and computed (at the GIAO/B3LYP/6-311++G(2d,p) level of theory) chemical shifts were obtained with a large set of 43 compounds in CHCl₃ exhibiting intramolecular O–H---O and intermolecular and intramolecular ionic O–H--- \bar{O} hydrogen bonds. The calculated OH chemical shifts exhibit a strong linear dependence on the computed (O)H---O hydrogen bond length, in the region of 1.24 to 1.85 Å, of -19.8 ppm Å⁻¹ and -20.49 ppm Å⁻¹ with optimization of the structures at the M06-2X/6-31+G(d) and B3LYP/6-31+G(d) level of theory, respectively. A Natural Bond Orbitals (NBO) analysis demonstrates a very good linear correlation between the calculated ¹H chemical shifts and (i) the second-order perturbation stabilization energies, corresponding to charge transfer between the oxygen lone pairs and σ_{OH}^* antibonding orbital and (ii) Wiberg bond order of the O–H---O and O–H--- \bar{O} hydrogen bond. Accurate *ab initio* calculations of O–H---O and O–H--- \bar{O} ¹H chemical shifts can provide improved structural and electronic description of hydrogen bonding and a highly accurate measure of distances of short and strong hydrogen bonds.

Keywords: *Ab initio*; hydrogen bonding; proton chemical shifts; natural bond orbital (NBO); resonance assisted hydrogen bond (RAHB)

Introduction

Hydrogen bonding is a fundamental aspect of chemical structure, conformation and reactivity.¹⁻⁹ Hydrogen bonding of *e.g.* OH---O, OH---N, NH---O, and NH---N groups, is a key interaction that determines the three dimensional structures in proteins, including enzymes and antibodies, and nucleic acids. The hydrogen bond is considered also of crucial importance in many biochemical processes by contributing to reactivity and transition state stabilization, proton transfer and tunneling and ligand binding specificity. The strength of a hydrogen bond depends on the H---Y length, the geometry of the X-H---Y-Z dihedral angle, the nature of its microenvironment, and the degree of matching of the pK_a values of the conjugate acids of the heavy atoms sharing the hydrogen.

Hydrogen bonds in proteins are generally in the range of 2.7 to 3.0 Å. However, in specific cases, short and strong hydrogen bonds or lower-barrier hydrogen bonds have been proposed to contribute significantly to the catalytic power of some enzymes by stabilizing the transition state or some labile intermediate.¹⁰ They are shorter (2.5 to 2.7 Å) and stronger (<-7 Kcal/mol) than normal hydrogen bonds and are predicted to enhance catalytic rates by more than 10⁴-fold. These hydrogen bonds are very controversial because it is difficult to distinguish experimentally a short and strong hydrogen bond that is 2.5 - 2.6 Å in length from a conventional hydrogen bond that is 2.7 to 3.0 Å in length, i.e. a difference of about 0.2 Å.

Detection of hydrogen bonds remains an area of active research. NMR spectroscopy is one of the most powerful methods for investigating hydrogen bonding interactions both in solution¹¹⁻¹³ and in the solid.^{14,15} The existence of a hydrogen bond is inferred by several NMR parameters and methods such as:

- (1) Chemical shifts. It has been established that the NMR chemical shift is a very sensitive indicator of hydrogen-bonding strength. For example clear correlations between ¹H solid-state NMR chemical shifts and OH---O hydrogen-bonding distance from X-ray and neutron crystallography structures were presented.¹⁶⁻²² These correlations have already been used for the characterization of strong and short hydrogen bonds in biological systems.²³⁻²⁶
- (2) Temperature dependence of chemical shift. Amide protons in peptide/proteins^{27,28} or hydroxyl OH protons of carbohydrates²⁹⁻³¹ and phenol OH protons of natural products^{13, 32, 33} involved in an intermolecular hydrogen bond show very strong temperature dependence (~-12 ppb/°C) whereas those involved in an intramolecular hydrogen bond have markedly lower temperature dependence (<-6 ppb/°C).
- (3) Protection of chemical exchange. The rate at which an intramolecularly hydrogen bonded amide proton in a protein disappears when the protein is dissolved in D₂O is markedly lower than in an amide proton hydrogen bonded with the solvent.³⁴
- (4) The nuclear Overhauser effect (NOE) which arises from dipole-dipole relaxation between spin ½ nuclei and is dependent on the distance between the nuclei and their motions.³⁵

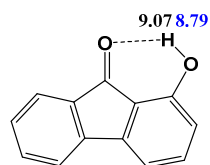
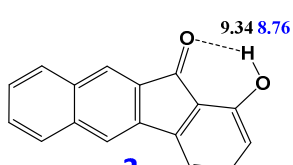
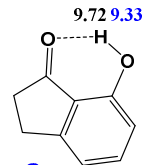
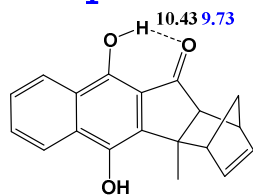
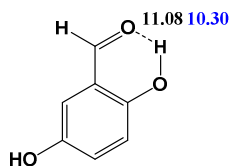
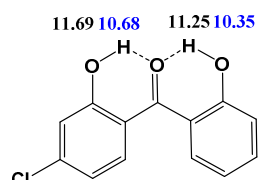
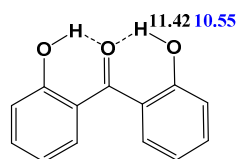
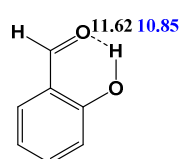
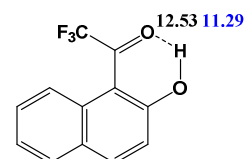
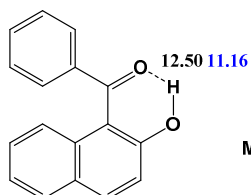
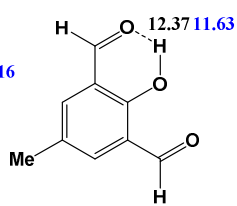
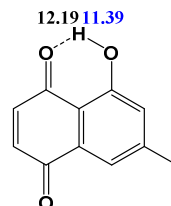
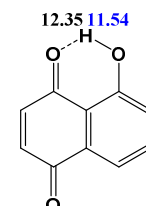
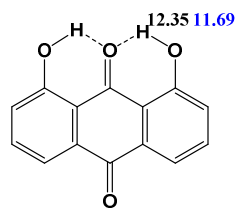
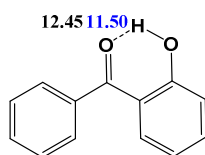
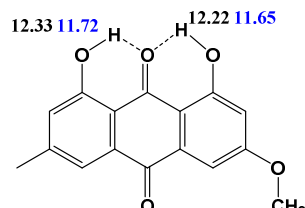
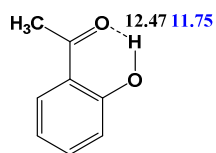
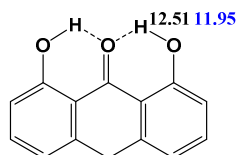
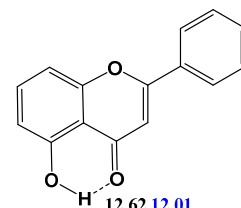
(5) Direct, across hydrogen bonds, spin-spin scalar couplings between nuclei on both sides of the hydrogen bond. This has been accomplished for nucleic acids and proteins^{36,37} and, to a limited extent, in carbohydrates.³⁸

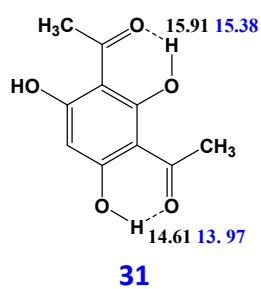
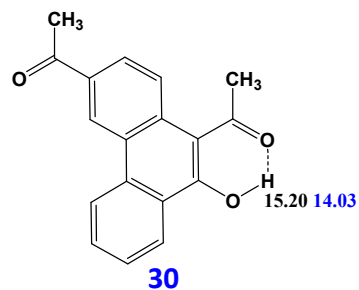
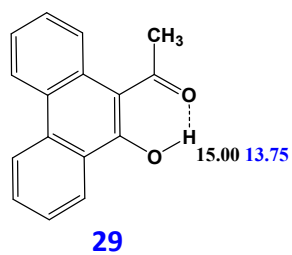
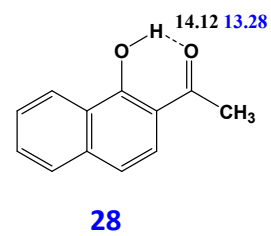
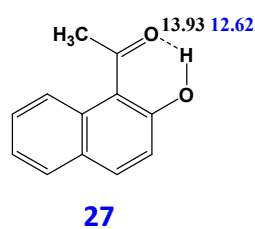
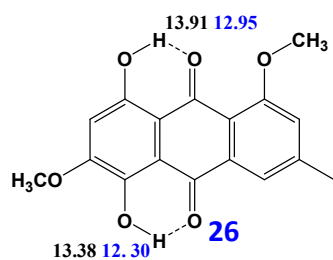
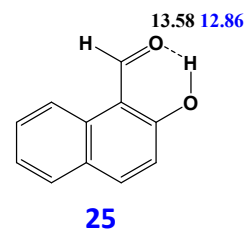
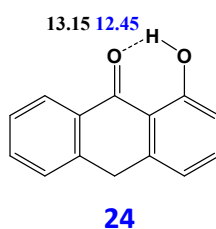
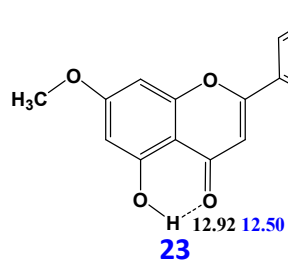
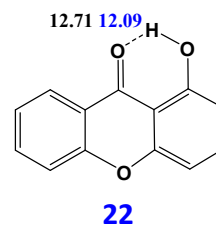
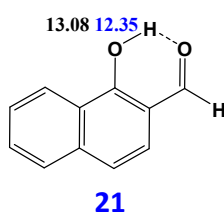
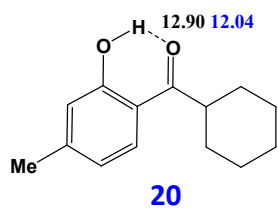
(6) REDOR experiments, which are an attractive tool for studies of hydrogen bonding in the solid.³⁹ This technique has been used to characterize α -helix structures in polypeptides by measuring $^{13}\text{C}=\text{O}\cdots^1\text{H}-^{15}\text{N}$ hydrogen bond lengths.⁴⁰

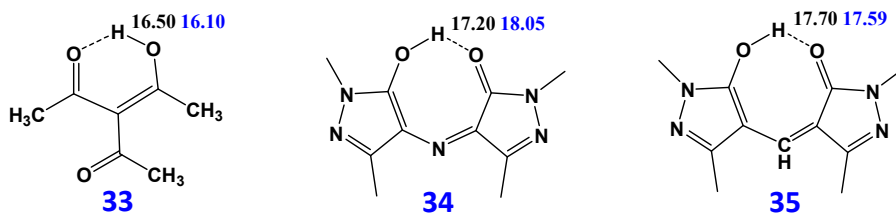
In recent years, developments in first-principles methods for calculating NMR parameters, with particular emphasis on chemical shifts^{41,42} as well as advances in computer power, have led to an increasing number of studies that combine calculation and experiment, thus allowing systematic investigations of hydrogen-bonding interactions.⁴³⁻⁴⁸ We report therein computed ^1H chemical shifts of a large set thirty five compounds exhibiting intramolecular $\text{O}-\text{H}\cdots\text{O}$ hydrogen bond and eight compounds exhibiting strong intramolecular and intermolecular ionic $\text{O}-\text{H}\cdots\text{O}^-$ hydrogen bonds with the combined use of DFT and conductor-like polarized continuum model (PCM) theory in CHCl_3 . The choice of the compounds has been dictated by the fact that the hydrogen bonding state of hydroxyl protons was shown to be a key factor in determining short and strong hydrogen bonds of molecules of biological interest.²³⁻²⁶

Results and discussion

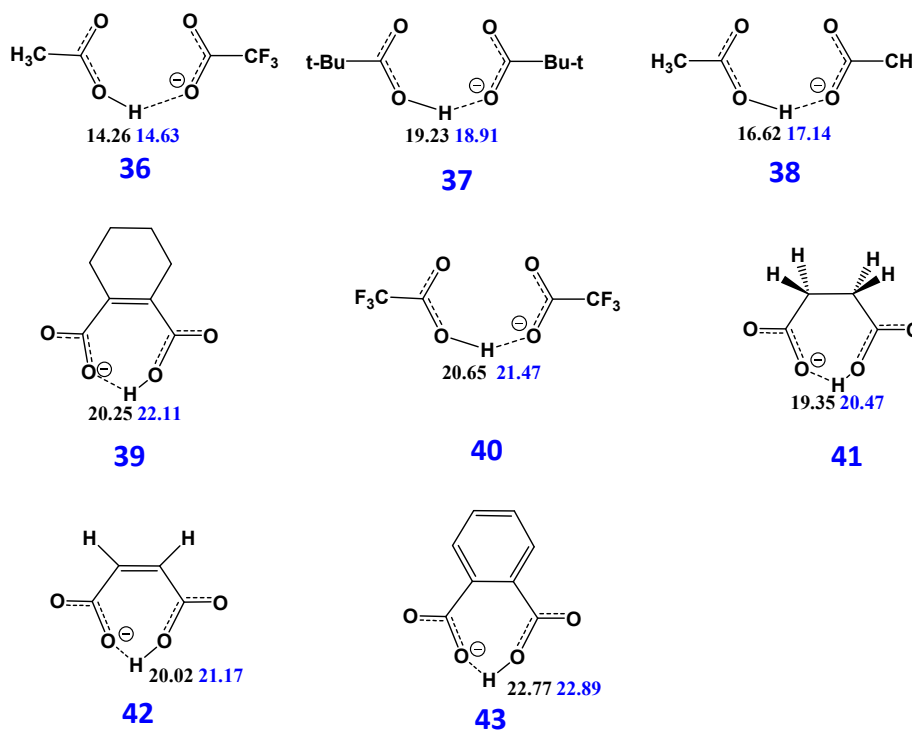
The use of hydroxyl proton chemical shifts in hydrogen bonding and conformational NMR studies in solution, presents experimental challenges due to rapid chemical exchange between hydroxyl groups and protic solvents. Proton exchange rates in $-\text{OH}$ groups can be significantly reduced in the presence of $\text{O}-\text{H}\cdots\text{O}$ intramolecular hydrogen bonds,^{13,32,33} by dissolving in $\text{DMSO}-d_6$ or acetone- d_6 ,²⁹ by supercooling aqueous solutions³⁰ or by using organic co-solvents³¹ and, thus, have already been utilized in structural analysis of carbohydrates^{31,46} and natural products.^{13,32,33} Furthermore, hydrogen bonded anions $\text{A}\cdots\text{H}\cdots\text{X}^-$ of phenols (AH) and carboxylic/inorganic acids (HX) have been extensively investigated.⁴⁹⁻⁵¹ Individual hydrogen bonded species in the slow NMR exchange regime were detected by the use of very low temperatures (120 K in $\text{CDF}_3/\text{CDF}_2\text{Cl}$ ⁵²). Therefore, a large set of experimental chemical shifts of test samples exist in the literature which can be used for evaluating *ab initio* prediction of $\text{O}-\text{H}\cdots\text{O}$ and $\text{O}-\text{H}\cdots\text{O}^-$ proton NMR chemical shifts (Scheme 1).

**1****2****3****4****5****6****7****8****9****10****11****12****13****14****15****16****17****18****19**





Anions



Scheme 1 Chemical formulas of phenol compounds exhibiting intramolecular O–H---O hydrogen bonds and ionic complexes with intramolecular and intermolecular O–H---O hydrogen bonds investigated in the present work. The data in black and blue are the computed ^1H chemical shifts, ppm, with minimization of the structures at the B3LYP/6-31+G(d) and M06-2X/6-31+G(d) level of theory, respectively (see Table 2).

Ab initio calculated vs experimental isotropic ^1H chemical shifts – effects of basis set

Siskos *et al.*⁴⁷ performed extensive calculations with the contactor-like polarizable continuum model (PCM)⁴⁵ and PCM discrete phenol + solvent hydrogen bonded complexes. The DFT method with the B3LYP hybrid functional⁵³ 6-31G(d), 6-31+G(d) and 6-311++G(d,p) basis set, as implemented in the Gaussian 03 package, resulted in excellent improvement of the calculated OH chemical shift when using discrete PhOH + solvent complexes. On the

contrary, an attempt to investigate the interaction of a solvent molecule, like CHCl_3 , CH_3CN , acetone and DMSO with the C-5 OH group of genkwanin, compound **23** in Scheme 1, by the use of DFT calculations was unsuccessful. The solvent molecule was displaced at a distance greater than 4 Å due to the formation of a strong intramolecular C-5 OH --- OC-4 hydrogen bond. Similar results were obtained, in the present work, for compounds **1**, **3** and **12** (Scheme 1). Therefore, a combination of the GIAO and the PCM methods with the B3LYP/6-311++G(2d,p) functional, as implemented in the Gaussian 09W package,⁵⁴ was used by minimizing the structures with the B3LYP/6-31+G(d) and M06-2X/6-31+G(d) basis sets without incorporating discrete solvent molecules. The computed geometries were then verified as minima by frequency calculations at the same level of theory (no imaginary frequencies). To convert ^1H NMR chemical shifts to the ppm scale, the isotropic $\delta(^1\text{H})$ values of tetramethylsilane (TMS), calculated at the same level of theory, were subtracted from the $\delta(\text{OH}, \text{ppm})$ values of the compounds under investigation.

A planar intramolecular hydrogen bond was observed for the compounds **1-5**, **8**, **11-14**, **16-26**, **28**, **31-35**, **39**, **41-43** (Scheme 1) with dihedral angles $\phi_1 = (\text{C})\text{O}-\text{H}---\text{O}=\text{C}$ and $\phi_2 = \text{C}-\text{O}-\text{H}---\text{O}(\text{C})$, deviating less than 1 degree. The benzophenone derivatives **6**, **7** and **15** deviate from planarity due to repulsive stereochemical interactions of the *ortho*-hydrogens of the phenyl groups [**6** with $\phi_1 = -10.93^\circ$ and -10.77° and $\phi_2 = -6.67^\circ$ and -7.21° (B3LYP/6-31+G(d)) and $\phi_1 = -12.69^\circ$ and -12.96° and $\phi_2 = -6.56^\circ$ and -6.94° (B06-2X/6-31+G(d)), **7** with $\phi_1 = -10.71^\circ$ and $\phi_2 = -7.12^\circ$ (B3LYP/6-31+G(d)) and $\phi_1 = -12.62^\circ$ and $\phi_2 = -7.00^\circ$ (M06-2X/6-31+G(d)), **15** with $\phi_1 = 4.23^\circ$ and $\phi_2 = 5.39^\circ$ (B3LYP/6-31+G(d)) and $\phi_1 = 5.93^\circ$ and $\phi_2 = 6.15^\circ$ (M06-2X/6-31+G(d)). The other classes of compounds with ϕ angles deviating from planarity are the 1-acylo-2-hydroxynaphthalenes [**9** with $\phi_1 = -5.28^\circ$ and $\phi_2 = 15.02^\circ$ (B3LYP/6-31+G(d)) and $\phi_1 = -2.61^\circ$ and $\phi_2 = 15.12^\circ$ (B06-2X/6-31+G(d)), **10** with $\phi_1 = 3.56^\circ$ and $\phi_2 = 13.53^\circ$ (B3LYP/6-31+G(d)) and $\phi_1 = 6.71^\circ$ and $\phi_2 = 13.30^\circ$ (B06-2X/6-31+G(d)), **27** with $\phi_1 = 4.38^\circ$ and $\phi_2 = -12.22^\circ$ (B3LYP/6-31+G(d)) and $\phi_1 = -2.54^\circ$ and $\phi_2 = 13.36^\circ$ (B06-2X/6-31+G(d)), and the two acetyl phenanthrene derivatives **29** [$\phi_1 = -6.90^\circ$ and $\phi_2 = 14.60^\circ$ (B3LYP/6-31+G(d)) and $\phi_1 = 5.38^\circ$ and $\phi_2 = -15.27^\circ$ (B06-2X/6-31+G(d))], and **30** [$\phi_1 = -6.85^\circ$ and $\phi_2 = 14.29^\circ$ (B3LYP/6-31+G(d)) and $\phi_1 = -5.27^\circ$ and $\phi_2 = 15.00^\circ$ (B06-2X/6-31+G(d))].

The structural details of selected compounds of known X-ray structures are depicted in Fig. 1 and Table 1. The agreement between the optimized computed and the experimental crystal structure is excellent.

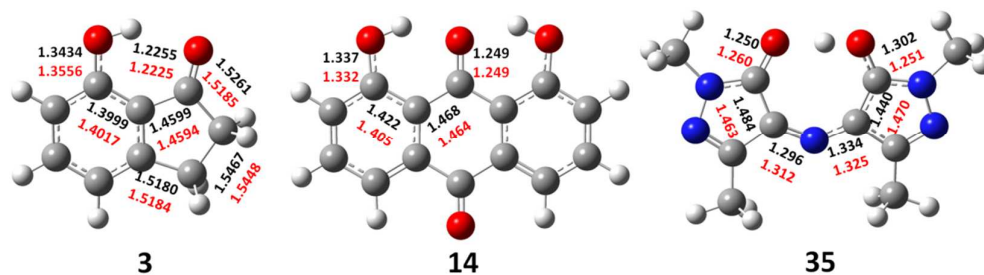


Fig. 1 Structures of the compounds **3**, **14** and **35** of Scheme 1 optimized at the M06-2X/6-31+G(d) level of theory. Calculated (in black) and experimental X-ray (in red) distances are expressed in Å.

Table 1 Comparison between calculated values of the hydrogen bond O-H...O geometry (Å and °) with data of the crystal structures for selected compounds of Scheme 1

Compd	O---O (Å)			O-H...O (Å) & O-H...O angle (degrees)		
	B3LYP/ 6-31+G(d)	M06-2X/ 31+G(d)	X-ray	B3LYP/ 6-31+G(d)	M06-2X/ 6-31+G(d)	X-ray
3	2.82613	2.84446	2.899(1) ⁵⁵	1.96789 144.1	2.00225 142.7	2.182(18) 138 ⁵⁵
8	2.65258	2.67242	2.6231(18) ⁵⁶	1.77701 145.5	1.81916 143.4	1.61 156 ⁵⁶
7	2.5993	2.63193	2.6061(11) ⁵⁷	1.69508 144.4	1.77197 142.0	1.88 144 ⁵⁷
14	2.58448	2.59765	2.538 -2.586 ⁵⁸	1.70550 145.6	1.74172 143.4	1.816-1.883 142 ⁵⁸
19	2.62181	2.63294	2.60 ⁵⁹	1.72324 147.9	1.75500 146.04	1.68 148 ⁵⁹
27	2.51257	2.54618	2.474 ⁶⁰	1.61806 146.35	1.68256 143.58	1.56 147 ⁶⁰
31	2.50517 2.47401	2.57297 2.51257	2.48 and 2.449 ⁶⁰	1.58832 1.53351 148.7 151.6	1.61450 1.55290 146.74 146.35	1.60-1.65 1.54 160 154-157 ⁶⁰
34	2.49111	2.46131	2.425 ⁶¹	1.44455 178.8	1.40867 178.8	1.306 177.0 ⁶¹
35	2.50176	2.48115	2.451 ⁶¹	1.46049 179.6	1.44083 178.2	1.400 166.8 ⁶¹

Table 2 illustrates calculated (δ , ppm) and experimental (δ_{exp} , ppm) ^1H chemical shifts, O-H and O...H bond distances, natural bond order (NBO) charges of the O...H-O atoms, and NBO charge differences of the two oxygens of the hydrogen bond ($\Delta Q \times 10^3$) of the compounds of Scheme 1. Fig. 2 shows the parity plot between experimental and calculated (with the GIAO method at the B3LYP/6-311++G(2d,p) level with PCM in CHCl_3) ^1H chemical shifts of the compounds **1** - **35** of Scheme 1 with minimization of the structures at the M06-2X/6-31+G(d) and the B3LYP/6-31+G(d) level of theory; the coefficients of linear regression R^2 of 0.965 and 0.977, respectively, show very good correlation between the calculated

isotropic chemical shifts of OH protons and the experimental chemical shifts. It may also be concluded that very large basis sets for energy minimization are not necessary to reproduce accurately ^1H NMR chemical shifts.

Further geometry optimizations were performed for the molecules **3**, **5**, **8** and **17** of Scheme 1 with the use of the computationally more demanding MP2/631 G+d level of theory which includes dispersion effects. The geometric characteristics and the calculated ^1H chemical shifts were found to be in very good agreement with those obtained at the B3LYP/6-311+G(d) and M06-2X/6-31+G(d) level of theory (Table S1). It can, therefore, be concluded that very large basis sets for energy minimization are not necessary to reproduce accurately ^1H NMR chemical shifts in agreement with literature data.⁸⁰

It should be emphasized that although hydrogen bonds presumably have substantial anharmonic character, the calculated ^1H chemical shifts of Table 2 were not corrected for quantum zero-point vibrational effects (QZPVE) for two reasons. First, detailed ^1H chemical shift correlations of water clusters $(\text{H}_2\text{O})_n$, $n=2$ to 16 using GIAO DFT methods demonstrated that QZPVE do not influence ^1H chemical shifts significantly and, thus, can be neglected.⁸¹ Second, detailed investigation of the temperature dependence of the chemical shifts, $\Delta\delta/\Delta T$, of phenol OH groups which participate in an intramolecular hydrogen bond demonstrated that $\Delta\delta/\Delta T$ values are very small, ≤ 3 ppb, in a variety of organic solvents with varying degrees of hydrogen bonding and solvation abilities. This implies a change of ^1H chemical shifts of ≤ 0.3 ppm for a temperature range of 100 K and, thus, a minor importance.

Table 2 Calculated (δ , ppm) GIAO/DFT/B3LYP/6-311+G(2d,p) (geometry optimization at the B3LYP/6-31+G(d) and M06-2X/6-31+G(d) level of theory) and experimental (δ_{exp} , ppm) ^1H chemical shifts, O---H and O-H bond distances, natural bond order (NBO) charges of the O---H-O atoms, and NBO charge differences of the two oxygens of the hydrogen bond ($\Delta Q \times 10^3$) of the compounds of Scheme 1

Compd	B3LYP/ 6-31+G(d) δ (ppm)	M06-2X/ 6-31+G(d) δ (ppm)	δ_{exp} (ppm)	O---H (Å)	O-H (Å)	NBO O---H-O	$\Delta Q \times 10^3$
1	9.07	8.79	8.76 ⁶²	2.04923	0.98315	(-0.578, +0.533, -0.690)	112
				2.07842	0.97824	(-0.572, +0.541, -0.706)	134
2	9.34	8.76	8-.64 ^{55,63}	2.02634	0.98385	(-0.588, +0.533, -0.691)	103
				2.05999	0.97875	(-0.579, +0.543, -0.706)	127
3	9.72	9.33	9.07, 9.04 ^{55,63}	1.96789	0.98563	(-0.604, +0.533, -0.693)	89
				2.00225	0.97982	(-0.601, +0.543, -0.709)	108
4	10.43	9.73	9.72 ⁶⁴	1.93876	0.98692	(-0.612, +0.537, -0.695)	83
				1.99843	0.98047	(-0.608, +0.547, -0.711)	103
5	11.01(49.65%) 11.15(50.35%) 11.08	10.08 (48.5%) 10.47(51.5%) 10.30	10.6 ⁶⁵	1.78342	0.98868	(-0.593, +0.533, -0.699)	106
				1.78486	0.98866	(-0.595, +0.533, -0.697)	102
				1.82655	0.97982	(-0.590, +0.544, -0.718)	128
				1.82531	0.98079	(-0.592, +0.545, -0.716)	124
6	11.25 11.69	10.35 10.68	10.43 10.81 ⁶⁶	1.73815	0.98692	(-0.672, +0.536, -0.696)	24
				1.72708	0.98862	(-0.672, +0.538, -0.692)	20
				1.79525	0.97878	(-0.667, +0.547, -0.714)	47
				1.78196	0.98027	(-0.667, +0.549, -0.710)	43
7	11.42	10.55	10.54 ^{67,68} 10.59 ^{66,69}	1.73187	0.98741	(-0.673, +0.536, -0.698)	25
				1.79045	0.97921	(-0.668, +0.547, -0.716)	48
8	11.62	10.85	11.01 ⁶⁵	1.77701	0.98985	(-0.596, +0.534, -0.693)	97
				1.81916	0.98173	(-0.595, +0.546, -0.712)	117

9	12.53	11.29	11.10 ⁷⁰	1.66898 1.74125	0.99237 0.98160	(-0582, +0.536, -0.678) (-0.576, +0.548, -0.699)	96 123
10	12.50	11.16	11.13 ⁷⁰	1.69508 1.77197	0.99237 0.98155	(-0.617, +0.537, -0.693) (-0.611, +0.548, -0.712)	76 101
11	12.37	11.63	11.45 ⁶⁹	1.75446 1.79817	0.99152 0.98306	(-0.588, +0.534, -0.657) (-0.587, +0.549, -0.679)	69 92
12	12.19	11.39	11.84 ⁶⁷	1.73269 1.77877	0.99280 0.98324	(-0.591, +0.536, -0.690) (-0.589, +0.548, -0.710)	99 121
13	12.35	11.54	11.86 ⁶⁷	1.73107 1.77694	0.99232 0.98291	(-0.586, +0.536, -0.689) (-0.584, +0.548, -0.710)	103 126
14	12.35	11.69	11.98 ⁶⁸	1.70550 1.74172	0.99079 0.98252	(-0.666, +0.538, -0.690) (-0.669, +0.549, -0.709)	24 40
15	12.45	11.50	12.02 ⁶⁷	1.69731 1.75040	0.99279 0.98318	(-0.611, +0.535, -0.698) (-0.608, +0.548, -0.717)	87 109
16	12.22 12.33	11.65 11.72	12.11 ⁷⁰ 12.32	1.70733 1.73743 1.70310	0.98130 0.98316 0.99197	(-0.674, +0.538, -0.694) (-0.678, +0.549, -0.711) (-0.674, +0.538, -0.693)	20 33 19
17	12.47	11.75	12.26, ^{70,72}	1.73576 1.69790 1.73631	0.98362 0.99348 0.98459	(-0.678, +0.549, -0.709) (-0.610, +0.534, -0.698) (-0.609, +0.547, -0.717)	31 85 108
18	12.51	11.95	12.23 ⁷⁰	1.68655 1.71821	0.99150 0.98338	(-0.679, +0.536, -0.697) (-0.585, +0.548, -0.714)	18 29
19	12.62	12.01	12.57 ⁷³	1.72324 1.75500	0.99693 0.98794	(-0.637, +0.536, -0.699) (-0.639, +0.549, -0.716)	42 77
20	12.90	12.04	12.61 ⁶⁶	1.66975 1.71307	0.99577 0.98607	(-0.624, +0.535, -0.700) (-0.621, +0.548, -0.718)	76 97
21	13.08	12.35	12.61 ^{70,72}	1.72608 1.76602	0.99522 0.98619	(-0.608, +0.538, -0.692) (-0.607, +0.552, -0.711)	84 104
22	12.71	12.09	12.56, 12.63 ^{74,75}	1.71940 1.75323	0.99448 0.98626	(-0.631, +0.535, -0.694) (-0.631, +0.548, -0.712)	63 81
23	12.92	12.50	12.89	1.72271 1.75509	0.99755 0.98830	(-0.631, +0.535, -0.694) (-0.644, +0.549, -0.716)	63 72
24	13.15	12.45	13.00 ⁷⁵	1.67646 1.71115	0.99547 0.98643	(-0.627, +0.534, -0.700) (-0.626, +0.547, -0.717)	73 91
25	13.58	12.86	13.15 ^{70,72}	1.68007 1.71520	0.99749 0.98807	(-0.610, +0.535, -0.687) (-0.610, +0.549, -0.708)	77 98
26	13.38 13.91	12.30 12.95	13.43 ⁷¹ 13.98	1.66846 1.72076 1.63738	0.99736 0.98570 1.00210	(-0.622, +0.536, -0.676) (-0.617, +0.549, -0.699) (-0.610, +0.537, -0.701)	54 82 89
27	13.93	12.62	13.93, 13.44 ^{70,72}	1.68097 1.61806 1.68256	0.98996 1.00022 0.98808	(-0.606, +0.551, -0.721) (-0.629, +0.536, -0.689) (-0.627, +0.550, -0.710)	115 60 83
28	14.12	13.28	14.11, 13.99 ^{70,72}	1.65192 1.69262	0.99990 0.98997	(-0.621, +0.538, -0.696) (-0.621, +0.553, -0.716)	75 95
29	15.00	13.75	14.61 ⁷⁰	1.59292 1.64796	1.00480 0.99260	(-0.634, +0.539, -0.692)	58
30	15.20	14.03	14.94 ⁷⁰	1.58712 1.63945	1.01611 0.99403	(-0.630, +0.539, -0.686) (-0.631, +0.555, -0.708)	56 77
31	14.61 15.91	13.97 15.38	14.5 ⁷⁰ 16.24 ⁷⁰	1.58832 1.61450 1.53351 1.55290	1.00792 0.99800 1.01518 1.00622	(-0.629, +0.538, -0.689) (-0.632, +0.553, -0.710) (-0.630, +0.539, -0.701) (-0.634, +0.555, -0.725)	60 78 71 91
32	16.76	16.49	17.09 ⁷⁶	1.5068 1.51752	1.02233 1.01495	(-0.629, +0.540, -0.692) (-0.635, +0.556, -0.717)	63 82
33	16.50	16.10	17.22 ⁷⁷	1.52904 1.54311	1.02208 1.01478	(-0.640, +0.538, -0.669) (-0.642, +0.554, -0.702)	29 60
34	17.20	18.05	17.3 ⁷⁸	1.46069 1.44083	1.04128 1.04060	(-0.693, +0.542, -0.696) (-0.707, +0.557, -0.723)	3 16
35	17.70	17.59	17.8 ⁷⁸	1.44455 1.40867	1.04669 1.05278	(-0.703, +0.542, -0.701) (-0.722, +0.557, -0.729)	-2 7
Anions							
36	14.34 ^a (8.2%) ^c 14.25 ^b (91.8%) ^c 14.26 ^d	16.82 ^a (1%) ^c 14.61 ^b (99%) ^c 14.63 ^d	14.57 ⁷⁹	1.56178 ^a 1.6277 ^b 1.50817a 1.60161b	1.03503 ^a 1.01526 ^b 1.04133a 1.01290b	(-0.754, +0.541, -0.755) (-0.758, +0.535, -0.748) (-0.772, +0.551, -0.781) (-0.781, +0.548, -0.776)	-1 10 -9 5
37	19.32 ^a (97.18%) ^c	20.78 ^a (46.01%) ^c	19.36 ⁷⁹	1.38308	1.10012	(-0.793, +0.535, -0.762)	-31

	16.11 ^b (2.82%) ^c	17.32 ^b (53.99%) ^c		1.55928 ^b	1.03303 ^b	(-0.817, +0.540, -0.748) ^b	-69
				1.29850	1.13567	(-0.810, +0.549, -0.792)	-18
	19.23 ^d	18.91 ^d		1.49879 ^b	1.04125 ^b	(-0.837, +0.551, -0.776) ^b	-51
38	18.96 ^a (11.87%) ^c	20.29(1.0%)	19.37 ⁷⁹	1.37708 ^b	1.10516	(-0.795, +0.538, -0.764)	-31
	16.30 ^b (88.13%) ^c	17.11 ^b (99%) ^c		1.53724 ^b	1.03931 ^b	(-0.808, +0.537, -0.755) ^b	-53
				1.29212	1.14240	(-0.810, +0.550, -0.793)	-17
	16.62 ^d	17.14 ^d		1.48775 ^b	1.04413 ^b	(-0.827, +0.548, -0.784) ^b	-43
39	20.25	22.11	19.90 ⁷⁹	1.40593	1.08017	(-0.743, +0.525, -0.764)	-22
				1.24084	1.13673	(-0.779, +0.540, -0.771)	-8
40	20.65	21.47	20.07 ⁷⁹	1.31074	1.13759	(-0.744, +0.530, -0.723)	-21
				1.23737	1.17881	(-0.764, +0.544, -0.758)	-6
41	19.35	20.47	20.27 ⁷⁹	1.40593	1.08017	(-0.792, +0.528, -0.762)	-30
				1.35039	1.09709	(-0.811, +0.543, -0.790)	-21
42	20.02	21.17	20.84 ⁷⁹	1.37790	1.08291	(-0.771, +0.526, -0.748)	-23
				1.31591	1.10506	(-0.790, +0.542, -0.774)	-16
43	22.77	22.89	21.33 ⁷⁹	1.19860	1.18586	(-0.746, +0.522, -0.747)	1
				1.19173	1.17940	(-0.772, +0.540, -0.770)	-2

^a Linear complex. ^b Bent complex. ^c Into parenthesis is the population (%) of the particular conformer.

^d Average chemical shift, δ_{av} , taking into consideration the populations of the two low energy conformers.

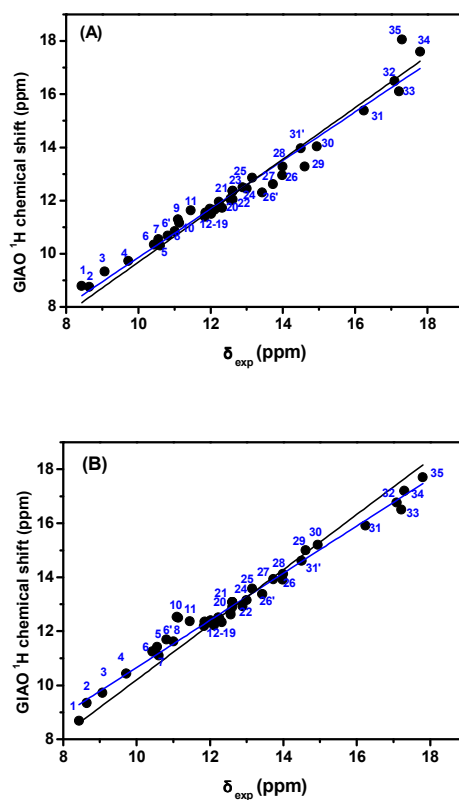


Fig. 2 Calculated (at the GIAO/B3LYP/6-311G+(2d,p) level of theory with PCM in CHCl_3) vs experimental chemical shifts of the OH protons of the compounds **1** - **35** of Scheme 1 with minimization of the structures at the M06-2X/6-31+G(d) (A) and B3LYP/6-31+G(d) (B) level of theory, respectively. The blue line corresponds to the linear fit and the black line to the linear fit through the zero.

Of particular interest are the ionic intermolecular hydrogen bonded structures **36** - **38** and **40**. The dimeric complex of CH_3COOH with CF_3COO^- , **36**, adopts two conformations: a bent one, with secondary attractive interactions between the carboxylate oxygen of the anion with the methyl group of CH_3COOH and a linear one (Fig. 3). The bent structure is more stable by about 1.43 kcal/mol with the B3LYP/6-31+G(d) and 2.73 kcal/mol with the M06-2X/6-31+G(d) basis set. Similarly, the dimeric charged complex **38** adopts two low energy conformers (1.19 and 2.73 kcal/mol) with the bent one being more stable due to attractive interactions between the carboxylate oxygen of the anion with the CH_3 groups. In the case of compound **37** (*t*-Bu group) the linear conformation was found to be more stable by 2.10 kcal/mol using the B3LYP/6-31+G(d) basis set while at the M06-2X/6-31+G(d) level of theory the bent conformer is slightly more stable than the linear one (0.095 kcal/mol). On the contrary, the dimeric charged complex **40** adopts a unique linear conformation since the bent one is of high energy due to the repulsive interaction between the carboxylate oxygen of the anion with the $-\text{CF}_3$ group. As expected, compounds **39**, **41**, **42** and **43** adopt a unique low energy conformer (Table 1). Inclusion in the analysis of the compounds **36** to **43** results also in very good linear correlation between experimental and computed chemical shifts with R^2 of 0.960 and 0.966 with optimization of the structures at the B3LYP/6-31+G(d) and M06-2X/6-31+G(d) level of theory, respectively (Fig. 4).

It should be emphasized that the computed average chemical shifts of the two low energy and, thus, more populated conformers of the complex **38** ($\delta_{\text{av}} = 16.62$ ppm at the B3LYP/6-31+G(d) and $\delta_{\text{av}} = 17.14$ ppm at the M06-2X/6-31+G(d) level of theory, Table 2) deviate significantly from the experimental value ($\delta = 19.37$ ppm). This deviation may be attributed to several reasons. First, hydrogen bond formation results in the appearance of several low-frequency normal vibrations describing relative motion of partner molecules, and chemical shifts of nuclei involved in a hydrogen bridge are very sensitive to hydrogen bond geometry.⁵² Second, the dielectric permittivity of solvents formed by dipolar molecules increases very rapidly with lowering the temperature due to molecular orientation, which can cause considerable alterations in geometry of highly polarizable hydrogen bonds. Third, more advanced basis sets are needed for the minimization of the intermolecular ionic hydrogen bonded complexes. Further calculations, therefore, were performed with minimization of the structures at the M06-2X/6-31+G(d) level of theory using a dielectric constant $\epsilon=40$ which was suggested to be an appropriate one for the low temperature (120K in $\text{CDF}_3/\text{CDF}_2\text{Cl}$) NMR experiments.⁵² Calculations demonstrated an increase in the internuclear hydrogen bond distance $\text{O-H}\cdots\text{O}$ presumably due to stabilization of the negative charge of the carboxylate group by solvation. Therefore, the intermolecular ionic hydrogen bond becomes weaker, thus, resulting in a decrease in the ^1H -NMR shifts and larger deviation from the experimental values. On the contrary, minimization of the structure with the more demanding B3LYP/6-311++G(p,d) level of theory, results in an increase in the average chemical shift ($\delta_{\text{av}}(\text{OH}) = 17.93$ ppm) and, thus, better agreement with the

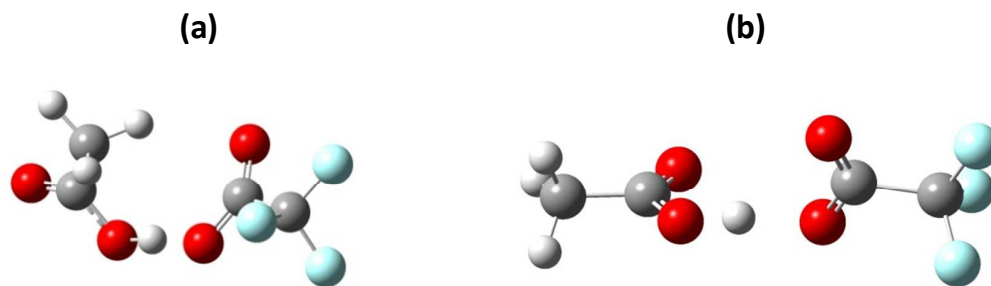


Fig. 3 Two low energy conformers of the complex $\text{CH}_3\text{COOH}\cdots\text{CF}_3\text{COO}$, **36**: (a) bent and (b) linear arrangement optimized at the M06-2X/6-31+G(d) level of theory.

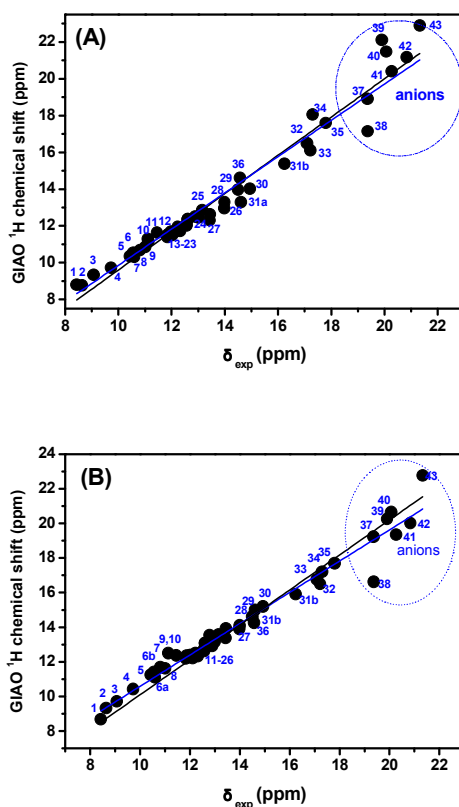


Fig. 4 Calculated (at the GIAO/B3LYP/6-311G+(2d,p) level of theory with PCM in CHCl_3) vs experimental chemical shifts of the OH protons of the compounds **1** - **43** of Scheme 1 with minimization of the structures at the M06-2X/6-31+G(d) (A) and B3LYP/6-31+G(d) (B) level of theory, respectively. The blue line corresponds to the linear fit and the black line to the linear fit through the zero.

experimental result ($\delta(\text{OH}) = 19.37$ ppm). The chemical shifts of the two low energy complexes were found to be $\delta(\text{OH}) = 20.47$ ppm for the linear conformer (35.96%) and

$\delta(\text{OH}) = 16.76$ ppm for the bent one (64%). It can, therefore, be concluded that for the intermolecular ionic hydrogen bonded complexes, high level basis set is required for the minimization of the structures due to delicate equilibrium of the two low energy conformers.

Calculated isotropic chemical shifts vs O---O, (O)H---O and O–H distances

Simple correlations between isotropic ^1H chemical shifts and O---H and O---O distances in O–H---O hydrogen bonds have been established for a variety of organic and inorganic solids.¹⁶ Thus, a linear relationship between isotropic ^1H chemical shift, $\delta(\text{OH})$ and O---O distance ($r_{\text{O---O}}$) has also been established for several metal phosphates and minerals⁸² and for carboxylic acid protons.⁸³

Bertolasi *et al.*⁷⁸ suggested a linear correlation between crystallographic $r(\text{O---O})$ distances and $\delta(\text{OH})$ ^1H chemical shifts of the form

$$\delta(\text{OH, ppm}) = -34.1 (\pm 2.6) r(\text{O---O}) (\text{\AA}) + 100.3 (\pm 64.0) \quad (1)$$

for a variety of molecules where the β -diketone enol group was found to form intramolecular O–H---O hydrogen bonds. A nearly linear relationship between the isotropic ^1H chemical shifts, $\delta(\text{OH})$, and H---O distance ($r_{\text{H---O}}$) has been presented¹⁸ for a series of compounds, using H---O distances determined from neutron diffraction (which are substantially more accurate than those determined from X-ray diffraction). The data were fitted well by a linear plot in which an increase of $r_{\text{H---O}}$ by 1.0 \AA corresponds to a change of $\delta(\text{OH})$ by -20 ppm. A linear relationship between $\delta(\text{OH})$ and $r_{\text{H---O}}$ was found over the whole range studied, from very short (almost symmetrical) hydrogen bonds to long hydrogen bonds (involving water molecules in hydrates).

Using structural data obtained from neutron diffraction studies for 41 different crystalline solids, the following linear relationship was reported²¹

$$\delta(\text{OH, ppm}) = 4.65 (r_{\text{H---O}}/\text{nm})^{-1} - 17.4 \quad (2)$$

For crystalline aminoacids a correlation of $r[(\text{O})\text{H---O}]$ hydrogen bond distances from X-ray diffraction with $\delta(\text{OH, ppm})$ from solid state NMR of the form

$$r[(\text{O})\text{H---O}] = 5.04 - 1.16 \ln \delta(\text{OH, ppm}) + 0.0447 \delta(\text{OH, ppm}) \quad (3)$$

was also suggested.²²

Fig. 5 illustrates the dependence of the computed OH proton chemical shifts, $\delta(\text{OH}, \text{ppm})$, of the compounds of Scheme 1 as a function of the computed O---O distances, Å. The resulting coefficient of linear regression R^2 demonstrates very poor correlation with minimization of the structures both at the M06-2X/6-31+G(d) and the B3LYP/6-31+G(d) level of theory. Compounds **1** to **4** (Scheme 1), which exhibit relatively weak hydrogen bonding, deviate significantly from a linear correlation. Furthermore, the anions **36** to **43** seems to present a separate class of compounds with an intercept of linear regression near parallel to that of compounds **5** to **35**. It has been suggested that O---O distances may not be sufficient indicators of hydrogen bond strength because the oxygen atoms can be thrust together due to steric and electronic constraints.⁸⁴ On the contrary, an excellent linear correlation of computed $\delta(\text{OH}, \text{ppm})$ vs computed (O)H---O, $r_{(\text{O})\text{H}\cdots\text{O}}$, hydrogen bond distances of the form

$$\delta_{\text{OH}} (\text{ppm}) = -19.83 r_{(\text{O})\text{H}\cdots\text{O}} + 46.49 \quad (R^2=0.986) \quad (4)$$

was obtained with a slope of $-19.83 \text{ ppm } \text{Å}^{-1}$ for minimization of the structures at the M06-2X/6-31+G(d) level of theory (Fig. 6A). Very good linear correlation of the form

$$\delta_{\text{OH}} (\text{ppm}) = -20.49 r_{(\text{O})\text{H}\cdots\text{O}} + 47.49 \quad (R^2=0.961) \quad (5)$$

with a slope of $-20.49 \text{ ppm } \text{Å}^{-1}$ was also obtained with minimization of the structures at the B3LYP/6-311+Gd level of theory (Fig. 6B).

Compounds **1** to **4** were not included in the linear regression analysis of Fig. 6 A,B since they deviate from linearity presumably because they exhibit relatively weak hydrogen bond with $R_{(\text{O})\text{H}\cdots\text{O}} > 1.9 \text{ Å}$. Similarly, non-linear behavior has been observed in CPCM calculations of discrete phenol + solvent hydrogen bonded complexes for $R_{(\text{O})\text{H}\cdots\text{O}} > 2.0 \text{ Å}$ ⁴⁷ and in *ab initio* calculations of acetone-phenol complexes at $R_{(\text{O})\text{H}\cdots\text{O}} > 2.1 \text{ Å}$.⁸⁵ Taking into consideration that the accuracy in estimating the slope in eqns (4) and (5) is 2 to 3%, it is evident that hydrogen bond distances with accuracy of $\pm 0.02 \text{ Å}$ to $\pm 0.03 \text{ Å}$ can be estimated for (O)H---O and (O)H---O hydrogen bonds in the range of 1.24 Å to 1.85 Å . It has been suggested that the accuracy in protein X-ray crystallography is $\sim 0.1 - 0.3 \times (\text{resolution})$, therefore, a structure with 2 Å resolution has standard errors in distances that are ± 0.2 to $\pm 0.6 \text{ Å}$. It can, therefore, be concluded that accurate *ab initio* calculations of O-H---O and O-H---O proton chemical shifts can provide a method for estimating hydrogen bond distances of labile protons beyond the limits of X-ray crystallography.

Fig. 7 illustrates calculated, at the GIAO/B3LYP/6-311+G(2d,p) level of theory with PCM in CHCl_3 , OH proton chemical shifts vs calculated elongation of the O-H bond of the structures

of the compounds of Scheme 1. The dependence is non-linear and the maximum elongation of the O-H bond is at ~ 1.24 Å which corresponds to computed chemical shifts of 21.96 ppm and 21.75 ppm for optimization of the structures at the B3LYP/6-31+G(d) and M06-2X/6-31+G(d) level of theory, respectively. These values should be compared with the experimental chemical shift of hydrogen maleate ($\delta = 20.82$ ppm) which was suggested to exhibit the strongest symmetric hydrogen bond where the hydrogen atom is near the midpoint of the donor and acceptor atoms and moves in a single well potential.^{79,86}

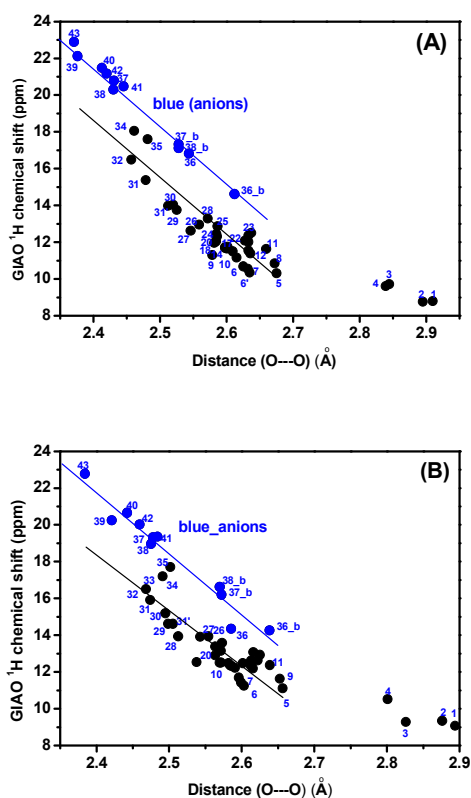


Fig. 5 Calculated ^1H chemical shifts [at the GIAO DFT/B3LYP/6-311+G(2d,p) level of theory with PCM (CHCl_3)] vs O...O distances of the compounds of Scheme 1 with minimization of the structures at the M06-2X/6-31+G(d) (A) and B3LYP/6-31+G(d) (B) level of theory.

Natural bond orbital analysis – the nature of hydrogen bonding

Table 2 represents the natural bond orbital (NBO) analysis of the compounds of Scheme 1 that has been carried out at the B3LYP/6-31+G(d) and M06-2X/6-31+G(d) level of theory. The NBO charge of the hydrogen participating in the intramolecular O-H...O or ionic O-H... $\bar{\text{O}}$ intra- and intermolecular hydrogen bond indicates an insignificant variation on the strength of hydrogen bonding in the whole range of the compounds **1-43** of Scheme 1. The charge of the proton acceptor oxygen increases from *e.g.* -0.578 for compound **1** up to -0.772 for compound **43** at the M06-2X/6-31+G(d) level of theory. The charge of the proton donor oxygen shows a moderate increase from -0.706 for compound **1** up to -0.770 for

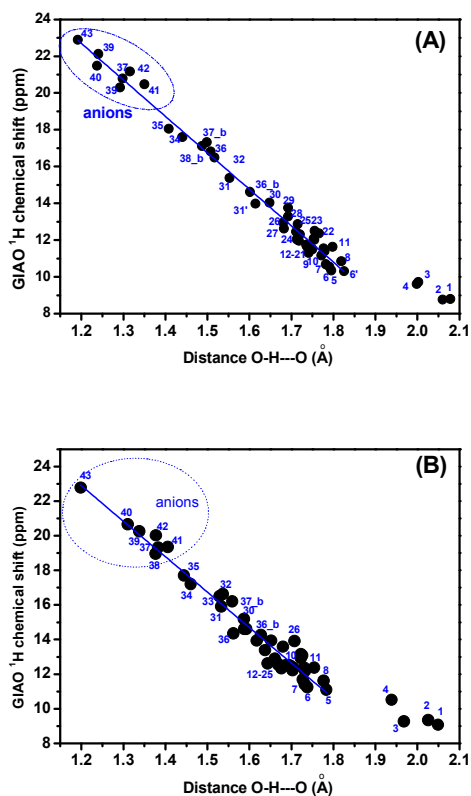


Fig. 6 Calculated (at the GIAO/B3LYP/6-311+ G(2d,p) level of theory with PCM in CHCl_3) OH proton chemical shifts vs calculated (O)-H---O distances, Å, of the compounds of Scheme 1 with minimization of the structures at the M06-2X/6-31+G(d) (A) and B3LYP/6-31+G(d) (B) level of theory.

compound **43** at the M06-2X/6-31+G(d) level of theory. Similar results were obtained at the B3LYP/6-31+G(d) level of theory. The difference in the magnitude of the NBO charges, $\Delta Q \times 10^3$, of the two oxygens participating in the intramolecular O-H---O or ionic O-H--- $\bar{\text{O}}$ intra- and intermolecular hydrogen bonding indicates no functional correlation with ^1H chemical shifts at the B3LYP/6-31+G(d) and M06-2X/6-31+G(d) level of theory (Fig. S1). Compounds **6**, **7**, **14**, **16** and **18** seem to form a particular class of compounds presumably due to the fact that two OH groups form intramolecular hydrogen bonding interactions simultaneously to the single CO group.

The O-H---O and O-H--- $\bar{\text{O}}$ hydrogen bond formation in terms of NBO analysis may be considered as a combination of two processes.^{87,88} The hyperconjugative interaction which is related to the charge transfer from the oxygen lone pair to the $\sigma^*(\text{O}-\text{H})$ antibonding orbital which leads to the elongation of the O-H bond and shortening of the O-H---O hydrogen bond. The second process is related to the increase in s-character of the oxygen hybrid

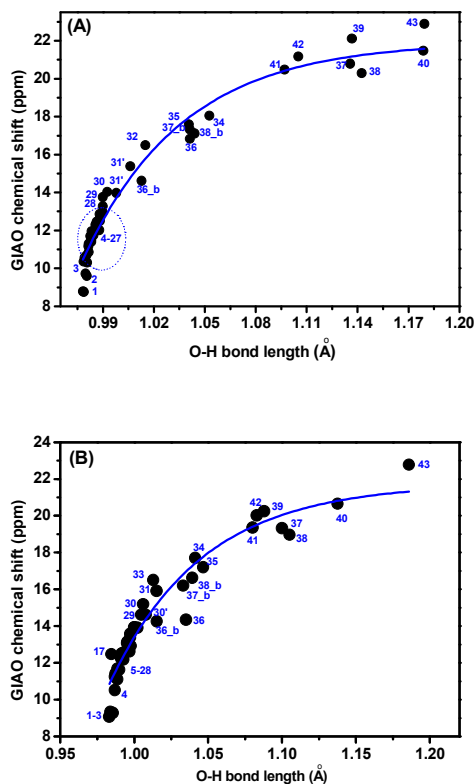


Fig.7 Calculated (at the GIAO/B3LYP/6-311+G(2d,p) level of theory with PCM in CHCl_3) OH proton chemical shifts vs calculated elongation of the O-H bond, Å, of the structures of the compounds of Scheme 1 optimized at the B3LYP/6-31+G(d) (A) and M06-2X/6-31+G(d) (B) level of theory.

orbital in the O–H bond and, thus, shortening of the O–H bond. In the NBO analysis of hydrogen bonded systems, the charge transfer process is considered to be the most important.

Fig. 8 shows second-order stabilization energies, $E^{(2)}$, corresponding to charge transfer between oxygen lone pair and σ_{OH}^* antibonding orbital [$E_{\text{LP}(\text{O}) \rightarrow \sigma_{\text{OH}}^*}^{(2)}$, in kcal mol^{-1}], as a function of the calculated ^1H chemical shifts of the compounds **1-35** of Scheme 1. The resulting coefficient of determination $R^2=0.946$ shows very good correlation between calculated ^1H chemical shifts and $E_{\text{LP}(\text{O}) \rightarrow \sigma_{\text{OH}}^*}^{(2)}$ which implies that the properties of charge transfer between the lone pairs of proton acceptor and the antibonding σ_{OH}^* of proton donor could be very useful to estimate the electronic properties and, thus, strength of intramolecular hydrogen bond. The value of $E_{\text{LP}(\text{O}) \rightarrow \sigma_{\text{OH}}^*}^{(2)}$ depends on at least two factors: (i) the hydrogen bond distance O---H(O) and (ii) the donor ability of the oxygen atom. The resulting excellent correlation between $\delta(\text{OH}, \text{ppm})$ and O---H(O) hydrogen bond distance (Fig. 6) implies that the factor (i) is the primary one in determining the $E_{\text{LP}(\text{O}) \rightarrow \sigma_{\text{OH}}^*}^{(2)}$ value.

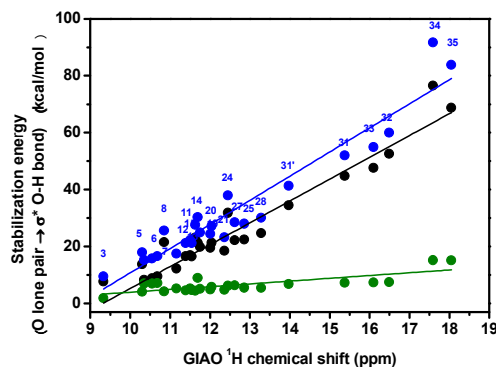


Fig. 8 Calculated (at the GIAO DFT/B3LYP/6-311+G(2d,p)] level of theory with PCM in CHCl_3) chemical shifts of the compounds of Scheme 1 with minimization of structures at the M06-2X/6-31+G(d) level of theory) vs stabilization energy (Second Order Perturbation Theory Analysis) between the lone pairs of the oxygen of the carbonyl group with the σ^* antibonding orbital of the H-O bond) (lone pair 1 in black, $R^2=0.946$, lone pair 2 in green, $R^2=0.575$, and the sum in blue, $R^2=0.921$).

Fig. 9 presents the NBO orbitals of the lone pair of the electron donor oxygen and the antibonding σ_{OH}^* of the acceptor OH group for three representative compounds of widely different second-order perturbation stabilization energies $E_{\text{LP(O)} \rightarrow \sigma_{\text{OH}}^*}^{(2)}$: the relatively weak interaction ($9.46 \text{ kcal mol}^{-1}$) of **3**, the moderate interaction ($24.43 \text{ kcal mol}^{-1}$) of **19**, and the strong one ($83.79 \text{ kcal mol}^{-1}$) of compound **35**. The significant delocalization within the extended π -system is also apparent especially for compound **35** (see discussion below).

The case of resonance assisted hydrogen bonding (RAHB)

The concept of “resonance-assisted hydrogen bond”⁸⁹ has been highlighted in numerous experimental and theoretical investigations.⁸⁹⁻⁹⁴ According to Gilli *et al.*^{89,90} the strength of the hydrogen bond is related to the π electron delocalization due to the mesomeric effect within the conjugated $\text{O}=\text{C}-\text{C}=\text{C}-\text{O}-\text{H}$ β -diketone enol group. This induces partial charges of opposite signs of the two oxygens resulting in a displacement of the hydrogen towards the keto oxygen group. The interplay, therefore, between hydrogen bond and heteroconjugated systems can strengthen significantly the hydrogen bond which lengthens the O–H bond and shortens both the O...H and the O...O distances. Madsen *et al.*^{95,96} introduced a modified model of the RAHB mechanism that allows the presence of partial positive charge on hydrogen and partial negative charges on both oxygens. This modified model, therefore, can

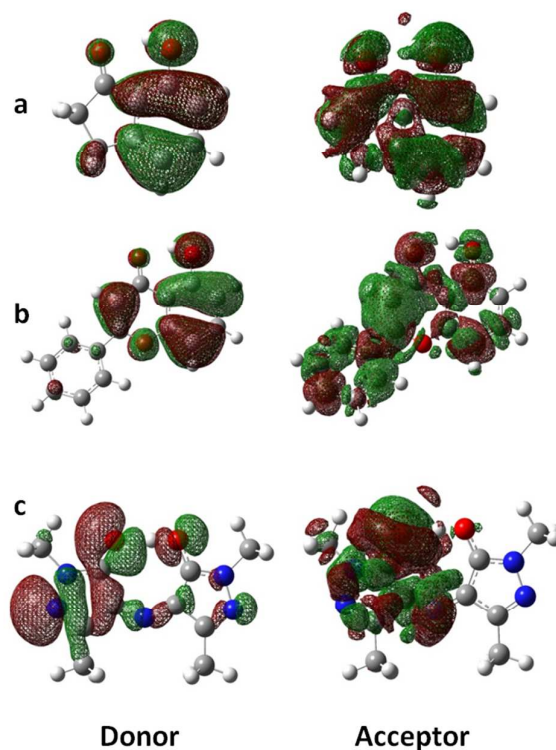


Fig. 9 The NBO donor-acceptor orbital of the lone pair 1 of the electron donor (proton acceptor) oxygen and the antibonding σ_{OH}^* of the acceptor (proton donor) group of the intramolecular hydrogen bond of the compounds **3** (a), **19** (b) and **35** (c).

be considered as an interplay of the original RAHB concept and a feedback mechanism that redistributes negative charge from the hydrogen onto the enol oxygen atom and the charges in the ring toward symmetry. The RAHB concept has been criticized by Alkorta *et al.*⁹⁷ on the basis of the coupling constants and proton chemical shifts and supported by Zarycz and Provacsi⁹⁸ on the basis of a localized molecular orbital (LMO) decomposition of the spin-spin coupling constants between atoms either involved or close to the O–H---O system of some β -diketones.

Table 3 illustrates the distribution of Wiberg bond order within the conjugated ring system. Fig. 10 demonstrates very good linear correlation between the GIAO calculated $\delta(^1\text{H})$ and Wiberg bond order of the intramolecular O---H(O) hydrogen bond of the compounds **1-35** of Scheme 1. Similar plot of the calculated Wiberg bond order of the CO group of the intramolecular CO---H(O) hydrogen bond vs GIAO calculated $\delta(^1\text{H})$ shows no functional relationship (Fig. S2). Nevertheless, the significant changes in the bond order (Table 3) and charge (Table S2) for various atoms of the ring system of compounds **1-35** is in agreement with the modified model of Madsen *et al.*^{95,96} and the concept that the RAHB redistributes the negative charge on both oxygens and the charges and bond orders within the ring system. The present quantitative analysis, which has advantages with regard to a classical valence bond order model used to describe OHO hydrogen bond geometries on the

basis of ^1H chemical shifts,^{79,86} clearly demonstrates that the O---H(O) Wiberg bond order is the dominant factor for determining the ^1H chemical shift and not the charge on the proton participating in hydrogen bonding.

Table 3 Wiberg bond order within the intramolecular hydrogen bonded moiety of the compounds **1-35** of Scheme 1. Minimization of the structures and the NBO analysis were performed at the M06-2X/6-31G+G(d) (blue) and B3LYP/6-31+G(d) (black) level of theory

Compound	C ₂ =O ₁	C ₂ -C ₃	C ₃ -C ₄	C ₄ -O ₅	O ₅ -H ₆	O ₁ ---H ₆
1	1.7302	1.0334	1.3308	1.0738	0.6671	0.0247
	1.6872	1.0573	1.3201	1.0841	0.6654	0.0344
2	1.7185	1.0416	1.3229	1.0783	0.6647	0.0263
	1.6706	1.0650	1.3056	1.0850	0.6623	0.0371
3	1.7265	1.0690	1.2834	1.0834	0.6575	0.0319
	1.6925	1.0994	1.2715	1.0944	0.6547	0.0441
4	1.7111	1.0798	1.3915	1.0793	0.6516	0.0320
	1.6711	1.1137	1.3579	1.0921	0.6454	0.0484
5	1.6727	1.1128	1.3584	1.0921	0.6465	0.0473
	1.7371	1.0920	1.2952	1.0820	0.6382	0.0501
6	1.6956	1.1307	1.2746	1.0993	0.6309	0.0690
	1.5820	1.0729	1.2989	1.0896	0.6391	0.0457
7		1.0713	1.2928	1.0977	0.6333	0.0490
	1.5178	1.1037	1.2800	1.1062	0.6245	0.0656
8		1.1011	1.2751	1.1134	0.6300	0.0694
	1.5834	1.0711	1.2999	1.0890	0.6377	0.0469
9	1.5187	1.1016	1.2811	1.1057	0.6284	0.0674
	1.6939	1.0733	1.2967	1.1022	0.6199	0.0645
10	1.6541	1.1063	1.2783	1.1184	0.6126	0.0850
	1.6963	1.1267	1.3616	1.1235	0.6238	0.0577
11	1.6379	1.1743	1.3187	1.1452	0.6086	0.0857
	1.6706	1.0615	1.3979	1.0996	0.6294	0.0526
12	1.6141	1.1000	1.3575	1.1212	0.6137	0.0806
	1.7349	1.0960	1.2864	1.1393	0.6283	0.0551
13	1.6961	1.1322	1.2691	1.1599	0.6214	0.0751
	1.6655	1.0764	1.3115	1.1050	0.6264	0.0570
14	1.6120	1.1072	1.2938	1.1222	0.6173	0.0788
	1.6730	1.0680	1.3133	1.1037	0.6268	0.0567
15	1.6198	1.0982	1.2965	1.1217	0.6177	0.0783
	1.5493	1.0855	1.3062	1.1043	0.6252	0.0576
16	1.4957	1.1154	1.2995	1.1198	0.6185	0.0761
	1.6711	1.0713	1.2956	1.0979	0.6242	0.0598
17	1.6238	1.1048	1.2758	1.1160	0.6135	0.0836
	1.5324	1.1020	1.2638	1.1029	0.6238	0.0595
18		1.0859	1.3031	1.1060	0.6227	0.0598
	1.4801	1.1313	1.2535	1.1171	0.6179	0.0770
19		1.1137	1.2924	1.1186	0.6164	0.0780
	1.6939	1.0733	1.3380	1.1022	0.6199	0.0645
20	1.6541	1.1063	1.3309	1.1184	0.6126	0.0850
	1.5330	1.0940	1.2749	1.1033	0.6211	0.0624
21	1.4858	1.1209	1.2618	1.1155	0.6157	0.804
	1.5985	1.0766	1.2613	1.1035	0.6154	0.0672
22	1.5566	1.0981	1.2547	1.1153	0.6099	0.0869
	1.6769	1.0832	1.2968	1.1049	0.6143	0.0688
23	1.6342	1.1180	1.2752	1.1212	0.6054	0.0915
	1.7023	1.1203	1.3637	1.1175	0.6150	0.0641
24	1.6614	1.1588	1.3301	1.1329	0.6083	0.0853
	1.6184	1.0941	1.2561	1.1053	0.6196	0.0643
25	1.5768	1.1199	1.2471	1.1183	0.6139	0.0838
	1.5893	1.0924	1.2231	1.1036	0.6150	0.0679
26	1.5444	1.1096	1.2222	1.1138	0.6096	0.0883

24	1.6326	1.0804	1.2745	1.1043	0.6146	0.0701
	1.5877	1.1080	1.2608	1.1183	0.6072	0.0909
25	1.6894	1.1298	1.3642	1.1237	0.6090	0.0729
	1.6496	1.1681	1.3291	1.1406	0.6018	0.0944
26	1.6342	1.0880	1.3913	1.1105	0.6153	0.0670
	1.6199	1.0902	1.3553	1.1056	0.6003	0.8000
	1.5756	1.1198	1.3576	1.1323	0.6027	0.0933
27	1.5633	1.1207	1.3253	1.1241	0.5885	0.1063
	1.6645	1.0894	1.3809	1.1217	0.6053	0.0748
	1.6144	1.1307	1.3409	1.1432	0.5899	0.1049
28	1.6674	1.0930	1.3751	1.1214	0.6000	0.0773
	1.6264	1.1264	1.3422	1.1378	0.5924	0.1002
29	1.6005	1.1380	1.3902	1.1528	0.5761	0.1150
30	1.6480	1.0999	1.4219	1.1426	0.5852	0.0890
	1.6034	1.1357	1.3769	1.1631	0.5732	0.1172
31	1.6439	1.0966	1.2582	1.1493	0.5774	0.1001
	1.6227	1.1168	1.2709	1.1469	0.5523	0.1212
	1.6100	1.1259	1.2438	1.1625	0.5725	0.1208
32	1.5893	1.1470	1.2593	1.1631	0.5508	0.1397
	1.6146	1.1131	1.2623	1.1732	0.5346	0.1371
	1.5876	1.1375	1.2560	1.1853	0.5370	0.1523
33	1.6110	1.1185	1.4839	1.2059	0.5429	0.1295
	1.5703	1.1768	1.4113	1.2408	0.5453	0.1445
34	1.4051	1.0838	1.2077	1.1836	0.4772	0.1950
		1.4858	1.2939			
	1.4175	1.0878	1.2066	1.1892	0.5012	0.1878
35		1.4752	1.3048			
	1.4366	1.0234	1.1712	1.1782	0.4943	0.1773
		1.5555	1.3175			
	1.4337	1.0314	1.1607	1.1897	0.5094	0.1791
	1.5241	1.3416				

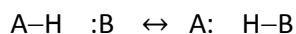
Conclusions

This paper provides the first extensive analysis of accurate *ab initio* calculations of O–H---O and ionic O–H---O⁻ proton chemical shifts of a large set of 43 compounds and complexes using a combination of DFT and polarizable continuum model (PCM). Several conclusions can be drawn from the present results:

(i) Excellent linear correlation between experimental and computed chemical shifts was obtained without using very large basis sets; however, for the intermolecular ionic O–H---O⁻ hydrogen bonded complexes high level basis set may be required for the minimization of the structures due to delicate equilibrium of low energy conformers.

(ii) The OH chemical shifts exhibit a strong linear dependence on the (O)H---O hydrogen bond length of -20.49 ppm Å⁻¹ at the M06-2X/6-31+G(d) and -19.8 ppm Å⁻¹ at the B3LYP/6-31+G(d) level of theory. This method, therefore, might be expected to be very effective in investigating hydrogen bonding effects on O–H---O and ionic O–H---O⁻ proton chemical shifts and in providing quantitative structural and electronic description of hydrogen bonding and accurate measure of distances of short and strong hydrogen bonds.

(iii) The NBO analysis provides strong evidence in support of the recent suggestion⁸⁸ for a revised definition of the hydrogen bond that is associated with the partial intra- and inter-molecular



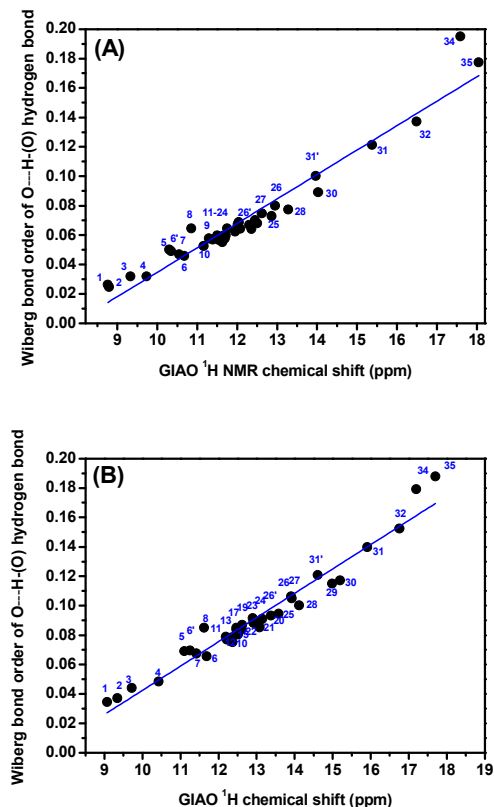


Fig. 10 Plot of calculated Wiberg bond order of the intramolecular O---H(O) hydrogen bond of the compounds **1-35** of Scheme 1 vs GIAO calculated ^1H chemical shifts. The minimization of the structures and the NBO analysis were performed at the M06-2X/6-31+G(d) (A) and the B3LYP/6-31+G(d) (B) level of theory.

three center/four electron proton sharing that originates mainly from a resonance type $n_{\text{B}} \rightarrow \sigma_{\text{AH}}^*$ interaction.

DFT calculations of OH proton chemical shifts, therefore, may be expected to contribute significantly to the current understanding of hydrogen bonding and might provide a highly sensitive measure of short and strong hydrogen bonds in biological systems that are inaccessible by the conventional X-ray crystallography. The term, therefore, of “NMR crystallography” that has only recently come into common usage^{99,100} can be extended in structural studies in the solution as well.

Conflict of interest

The authors declare no competing financial interests.

Acknowledgements

The authors thank Prof. S. Loukas, Department of Mathematics, University of Ioannina, for fruitful discussions and the anonymous reviewers for critical and constructive criticisms.

References and notes

- 1 G. A. Jeffrey and S. W. Sanger, *Hydrogen bonding in biological structures*. Springer Verlag, Berlin, 1991.
- 2 G. A. Jeffrey, *An introduction to hydrogen bonding*. Oxford University Press, New York, 1997.
- 3 S. Scheider, *Hydrogen bonding: a theoretical perspective*. Oxford University Press, New York, 1997.
- 4 (a) C. L. Perrin and J. B. Nielson, *Annu. Rev. Phys. Chem.*, 1997, **48**, 511-544; (b) C.L. Perrin, *Acc. Chem. Res.*, 2010, **43**, 1550-1557.
- 5 I. Alkorta, I. Rozas and J. Elguero, *Chem. Soc. Rev.*, 1998, **27**, 163-170.
- 6 G. R. Desiraju and T. Steiner, *The weak hydrogen bond in structural chemistry and biology*. Oxford: Oxford University Press, 1999.
- 7 T. Steiner, *Angew. Chem. Int. Ed.*, 2002, **41**, 49-76.
- 8 S. J. Grabowski (Ed.), Hydrogen bonding – new insights in *Challenges and Advances in Computational Chemistry and Physics*, Vol. 3. Springer, Dordrecht, 2005.
- 9 P. Gilli, L. Pretto, V. Bertolasi and G. Gilli, *Acc. Chem. Res.*, 2009, **42**, 33-44.
- 10 H. Ishikita and K. Saito, *J. R. Soc. Interface*, 2014, **11**, 20130518.
- 11 M. Blackledge, *Protein Sci.*, 2007, **16**, 1247-1248.
- 12 (a) I. P. Gerothanassis, *Progr. Nucl. Magn. Reson. Spectrosc.*, 2010, **56**, 95-197; (b) I. P. Gerothanassis, *Progr. Nucl. Magn. Reson. Spectrosc.*, 2010, **57**, 1-110.
- 13 P. Charisiadis, V. G. Kontogianni, C. G. Tsiafoulis, A. G. Tzakos, M. Siskos and I. P. Gerothanassis, *Molecules*, 2014, **19**, 13643-13682.
- 14 E. Brunner and U. Sternberg, *Progr. Nucl. Magn. Reson. Spectrosc.*, 1998, **32**, 21-57.
- 15 A. E. Aliev and K. D. M. Harris, *Structure and Bonding*, 2004, **108**, 1-53.
- 16 B. Berglund and R. W. Vaughan, *J. Chem. Phys.*, 1980, **73**, 2037-2043.
- 17 C. M. Rohlfing, I. C. Allan and R. Ditchfield, *J. Chem. Phys.*, 1983, **79**, 4958-4966.
- 18 G. A. Jeffrey and Y. Yeon, *Acta Crystallogr. B*, 1986, **42**, 410-413.
- 19 R. Kaliaperumal, R.E.J. Sears, Q.W. Ni and J.E. Furst, *J. Chem. Phys.*, 1989, **91**, 7387-7391.
- 20 H. Eckert, J. P. Yesinowski, L.A. Silver and E. M. Stople, *J. Phys. Chem.*, 1988, **92**, 2055-2064.
- 21 U. Sternberg and E. Brunner, *J. Magn. Reson. A*, 1994, **108**, 142-150.

- 22 A. Mc Dermott and C. F. Ridenour in *Proton Chemical Shift Measurements in Biological Solids. Encyclopedia of NMR*. Wiley, Sussex, UK, 1996, 3820-3825.
- 23 T. K. Harris and A. S. Mildvan, *Proteins: Structure, Function and Genetics*, 1999, **35**, 275-282.
- 24 T. K. Harris, Q. Zhao and A. S. Mildvan, *J. Mol. Struct.*, 2000, **552**, 97-109.
- 25 P. A. Sigala, J. M. M. Caaveiro, D. Ringe, G. A. Petsko and D. Herschlag, *Biochemistry*, 2009, **48**, 6932-6939.
- 26 P. A. Sigala, A. T. Fafarman, J. P. Schwans, S. D. Fried, T. D. Fenn, J. M. Caaveiro, B. Pybus, D. Ringe, G. A. Petsko, S. G. Boxer and D. Herschlag, *Proc. Natl. Acad. Sci. USA*, 2013, **110**, E2552-E2561.
- 27 N. J. Baxter and M. P. Williamson, *J. Biomol. NMR*, 1997, **9**, 359-369.
- 28 H. J. Dyson, M. Rance, R. A. Houghten, R. A. Lerner and P. E. Wright, *J. Mol. Biol.*, 1988, **201**, 161-200.
- 29 B. Casu, M. Reggiani, G. G. Gallo and A. Vigevani, *Tetrahedron*, 1966, **22**, 3061-3083.
- 30 L. Poppe and H. van Halbeek, *Nat. Struct. Biol.*, 1994, **1**, 215-216.
- 31 B. Adams and L. Lerner, *J. Am. Chem. Soc.*, 1992, **114**, 4827-4829.
- 32 V. Exarchou, V. Troganis, I. P. Gerotheranassis, M. Tsimidou and D. Boskou, *Tetrahedron*, 2002, **58**, 7423-7429.
- 33 V. G. Kontogianni, P. Charisiadis, A. Primikyri, C. G. Pappas, V. Exarchou, A. G. Tzakos and I. P. Gerotheranassis, *Org. Biomol. Chem.*, 2013, **11**, 1013-1025.
- 34 S.W. Englander and N.R. Kallenbach, *Q. Rev. Biophys.*, 1983, **16**, 521-655.
- 35 (a) D. Neuhaus and M. P. Williamson, *The nuclear Overhauser effect in structural and conformational analysis*, 2nd Ed. New York, Wiley – VCH, 2000; (b) B. Vögeli, *Progr. Nucl. Magn. Reson. Spectrosc.*, 2014, **78**, 1-46.
- 36 A. J. Dingley and S. Grzesiek, *J. Am. Chem. Soc.*, 1998, **120**, 8293-8297.
- 37 S. Grzesiek, F. Cordier and A. J. Dingley, *Methods Enzymol.*, 2002, **338**, 111-133.
- 38 M. Barfield, J. M. Bergset and D. J. O'Leary, *Magn. Reson. Chem.*, 2001, **39**, S115-S125.
- 39 A. Naito, K. Nishimura, S. Kimura, M. Aida, N. Yosuka, S. Tuzi and H. Saito, *J. Phys. Chem.*, 1996, **100**, 14995-15004.
- 40 S. Kimura, A. Naito, H. Saito, K. Ogawa and A. Shoji, *J. Mol. Struct.*, 2001, **562**, 197-203.
- 41 A. C. De Dios, *Prog. Nucl. Magn. Reson. Spectrosc.*, 1996, **29**, 229-278.
- 42 F. A. A. Mulder and M. Filatov, *Chem. Soc. Rev.*, 2010, **39**, 578-590.
- 43 G. A. Kumar and M. A. McAllister, *J. Org. Chem.*, 1998, **63**, 6968-6972.
- 44 R. K. Harris, P. Y. Ghi, R. B. Hammond, C. Y. Ma and K. J. Roberts, *Chem. Commun.*, 2003, 2834-2835.
- 45 R. A. Klein, B. Mennucci and J. Tomasi, *J. Phys. Chem. A*, 2004, **108**, 5851-5863.

- 46 S. Bekiroglu, A. Sandström, L. Kenne and C. Sandström, *Org. Biomol. Chem.*, 2004, **2**, 200-205.
- 47 M. Siskos, V. G. Kontogianni, C. Tsiafoulis, A. Tzakos and I. P. Gerothanassis, *Org. Biomol. Chem.*, 2013, **11**, 7400-7411.
- 48 A. Victora, H. M. Möller and T. E. Exner, *Nucl. Acids Res.*, 2014, **42**, e173.
- 49 P. M. Tolstoy, B. Koeppe, G. S. Denisov and H.-H. Limbach, *Angew. Chem. Int. Ed.*, 2009, **48**, 5745-5747.
- 50 B. Koeppe, P. M. Tolstoy and H.-H. Limbach, *J. Am. Chem. Soc.*, 2011, **133**, 7897-7908.
- 51 B. Koeppe, J. Guo, P. M. Tolstoy, G. S. Denisov and H.-H. Limbach, *J. Am. Chem. Soc.*, 2013, **135**, 7553-7566.
- 52 I. G. Shenderovich, A. P. Burtsev, G. S. Denisov, N. S. Golubev and H.-H. Limbach, *Magn. Reson. Chem.*, 2001, **39**, S91-S99.
- 53 A. D. Becke, *J. Chem. Phys.*, 1993, **98**, 5648-5652.
- 54 M. J. Frisch, G. W. Trucks, H. B. Schlegel, G. E. Scuseria, M. A. Robb, J. R. Cheeseman, G. Scalmani, V. Barone, B. Mennucci, G. A. Petersson, H. Nakatsuji, M. Caricato, X. Li, H. P. Hratchian, A. F. Izmaylov, J. Bloino, G. Zheng, J. L. Sonnenberg, M. Hada, M. Ehara, K. Toyota, R. Fukuda, J. Hasegawa, M. Ishida, T. Nakajima, Y. Honda, O. Kitao, H. Nakai, T. Vreven, J. A. Montgomery, Jr., J. E. Peralta, F. Ogliaro, M. Bearpark, J. J. Heyd, E. Brothers, K. N. Kudin, V. N. Staroverov, T. Keith, R. Kobayashi, J. Normand, K. Raghavachari, A. Rendell, J. C. Burant, S. S. Iyengar, J. Tomasi, M. Cossi, N. Rega, J. M. Millam, M. Klene, J. E. Knox, J. B. Cross, V. Bakken, C. Adamo, J. Jaramillo, R. Gomperts, R. E. Stratmann, O. Yazyev, A. J. Austin, R. Cammi, C. Pomelli, J. W. Ochterski, R. L. Martin, K. Morokuma, V. G. Zakrzewski, G. A. Voth, P. Salvador, J. J. Dannenberg, S. Dapprich, A. D. Daniels, O. Farkas, J. B. Foresman, J. V. Ortiz, J. Cioslowski, and D. J. Fox, *Gaussian 0.9, revision B.01*, Gaussian, Inc., Wallingford, CT, 2010.
- 55 K. Y. Chen, Y. S. Wen, T. C. Fang, Y. J. Chang and M. J. Chang, *Acta Cryst.*, 2011, **E67**, 927.
- 56 M. T. Kirchner, D. Blaser, R. Boese, T. S. Thakur and G. R. Desirajub, *Acta Cryst.*, 2011, **C67**, 387-390.
- 57 R. Betz, T. Gerber and H. Schalekamp, *Acta Cryst.*, 2011, **E67**, 1897.
- 58 A. L. Rohl, M. Moret, W. Kaminsky, K. Claborn, J. J. McKinnon and B. Kahr, *Cryst. Growth Des.*, 2008, **8**, 4517-4525.
- 59 M. Shoja, *Acta Cryst.*, 1990, **C46**, 517-519.
- 60 P. E. Hansen, S. Bolvig and K. Wozniak, *J. Mol. Struct.*, 2005, **749**, 155-168.
- 61 U. Drück and W. Littke, *Acta Cryst.*, 1980, **B36**, 3002-3007.
- 62 (a) K.-C. Tang, M.-J. Chang, T.-Y. Lin, H.-A. Pan, T.-C. Fang, K.-Y. Chen, W. Y. Hung, Y. H. Hsu and P. T. Chou, *J. Am. Chem. Soc.*, 2011, **133**, 17738-17745; (b) L. Minuti, A. Taticchi, A. Marrocchi, D. Lanari, A. Broggi and E. Gacs-Baitz, *Tetrahedron: Asymmetry*, 2003, **14**, 481-487.
- 63 A. A. Narine, PhD. Thesis, University of Simon Fraser, Canada, 2004, 171.
- 64 S. R. De, S. K. Ghorai and D. Mal, *J. Org. Chem.*, 2009, **74**, 1598-1604.

- 65 P. E. Hansen, *Magn. Reson. Chem.*, 1993, **31**, 23-37.
- 66 G. Shan, X. Han, Y. Lin, S. Yu and Y. Rao, *Org. Biomol. Chem.*, 2013, **11**, 2318-2322.
- 67 G. Jaccard and J. Lauterwein, *Helv. Chim. Acta*, 1986, **69**, 1469-1485.
- 68 Spectral Database for Organic Compounds SDBS, http://sdb.sdb.aist.go.jp/sdb/cgi-bin/cre_frame_disp.cgi?sdbno=4544.
- 69 P. E. Hansen and S. Bolving, *Magn. Reson. Chem.*, 1997, **35**, 520-528.
- 70 P. E. Hansen, S. N. Ibsen, T. Kristensen and S. Bolving, *Magn. Reson. Chem.*, 1994, **32**, 399-408.
- 71 M. Gill and P. M. Morgan, *ARKIVOC*, 2001, 145-156.
- 72 E. V. Borisov, W. Zhang, S. Bolving and P. E. Hansen, *Magn. Reson. Chem.*, 1998, **36**, S104-S110.
- 73 Y. Park, B. H. Moon, E. Lee, Y. Lee, Y. Yoon, J. H. Ahn and Y. Lim, *Magn. Reson. Chem.*, 2007, **45**, 674-679.
- 74 M. J. Carvalho, L. M. Carvalho, A. M. Ferreira and A. M. S. Silva, *Nat. Prod. Res.*, 2003, **17**, 445-449.
- 75 C. Commandeur, J.-C. Florent, P. Rousselle and E. Bertounesque, *Eur. J. Org. Chem.*, 2011, 1447-1451.
- 76 J. Abildgaard, S. Bolvig and P. E. Hansen, *J. Am. Chem. Soc.*, 1998, **120**, 9063-9069.
- 77 S. Bolving, F. Duus and P. E. Hansen, *Magn. Reson. Chem.*, 1998, **36**, 315-324.
- 78 V. Bertolasi, P. Gilli, V. Ferretti and G. Gilli, *J. Chem. Soc. Perkin Trans. 2*, 1997, **5**, 945-952.
- 79 J. Guo, P. M. Tolstoy, B. Koeppe, N. S. Golubev, G. S. Denisov, S. N. Smirnov and H.-H. Limbach, *J. Phys. Chem. A*, 2012, **116**, 11180-11188.
- 80 P.B. Karadakov, *J. Mol. Struct.*, 2002, **602-603**, 293-301.
- 81 H.-H. Limbach, P.M. Tolstoy, N. Perez-Hernandez, J. Guo, I.G. Shenderovich and G.S. Denisov, *Israel J. Chem.*, 2009, **49**, 199-2016.
- 82 J. P. Yesinowski and H. Eckert, *J. Am. Chem. Soc.*, 1987, **109**, 6274-6282.
- 83 R. K. Harris, P. Jackson, L. H. Merwin, B. J. Say and G. Hägele, *J. Chem. Soc. Faraday Trans.*, 1988, **84**, 3649-3672.
- 84 Y. H. Mariam and R. N. Musin, *J. Phys. Chem. A*, 2008, **112**, 134-145.
- 85 R. J. Abraham and M. Mobli, *Magn. Reson. Chem.*, 2007, **45**, 865-877.
- 86 P.M. Tolstoy, P. Schah-Mohammedi, S.N. Smirnov, N.S. Golubev, G.S. Denisov and H.-H. Limbach, *J. Am. Chem. Soc.*, 2004, **126**, 5621-5634.
- 87 A. E. Reed, L. A. Curtiss and F. Weinhold, *Chem. Rev.*, 1988, **88**, 899-926.
- 88 F. Weinhold and R. Klein, *Mol. Phys.*, 2012, **110**, 565-579.
- 89 G. Gilli, F. Bellucci, V. Ferretti and V. Bertolasi, *J. Am. Chem. Soc.*, 1989, **111**, 1023-1028.
- 90 V. Bertolasi, P. Gilli, V. Ferretti and G. Gilli, *J. Am. Chem. Soc.*, 1991, **113**, 4917-4925.

- 91 C. Fonseca Guerra, F. M. Bickelhaupt, J. G. Snijders and E. J. Baerends, *J. Am. Chem. Soc.*, 2000, **122**, 4117-4128.
- 92 A. Bouchy, D. Rinaldi and J. L. Rivail, *Int. J. Quantum Chem.*, 2004, **96**, 273-281.
- 93 Y. Mo, *J. Phys. Chem. A*, 2012, **116**, 5240-5246.
- 94 D. Rusinka-Roszak, *J. Phys. Chem. A*, 2015, DOI: 10.1021/acs.jpca.5b02343.
- 95 G. K. H. Madsen, B. B. Iversen, F. K. Larsen, M. Kapon, G. M. Reisner and F. H. Herbstein, *J. Am. Chem. Soc.*, 1998, **120**, 10040-10045.
- 96 B. Schiøtt, B. B. Iversen, G. K. H. Madsen and T. C. Bruice, *J. Am. Chem. Soc.*, 1998, **120**, 12117-12124.
- 97 I. Alkorta, J. Elguero, O. Mó, M. Yáñez and J. E. Del Bene, *Mol. Phys.*, 2004, **102**, 2563-2574.
- 98 M. N. C. Zarycz and P. F. Provasi, *Magn. Reson. Chem.*, 2015, **53**, 120-129.
- 99 R. K. Harris, R. E. Wasylshen and M. J. Duer (Eds.), *NMR Crystallography*, John Wiley & Sons, Chichester, 2009.
- 100 L. J. Mueller and M. F. Dunn, *Acc. Chem. Res.*, 2013, **46**, 2008-2017.